



Irina Gancheva<sup>1,2</sup>, Gordon Campbell<sup>1</sup>, Elisaveta Peneva<sup>2</sup>, Beniamino Abis<sup>3,4</sup>

<sup>1</sup> ESA - European Space Agency      <sup>3</sup> ESA-RSS (Research and Service Support)

<sup>2</sup> Sofia University "St. Kliment Ohridski"      <sup>4</sup> Progressive Systems Srl

Corresponding author: [Irina.Gancheva@esa.int](mailto:Irina.Gancheva@esa.int)

## Objective

Detection of the surface signature of riverine outflow with the further aim of detecting untreated or poorly treated sewage water discharges using satellite data.

## Challenges

Problems, related with remote waste water detection:

- Small scale events
- Strong influence of meteorological conditions
- Interaction with other local phenomena
- Interaction with the ambient water depends on the waste water constitution

## (Partial) Solution

Observe similar events and understand detection mechanism  
→ Observation of surface signature of river plumes

How riverine outflow in marine environment is similar to poorly treated waste water?

- Higher nutrient concentration
- High sediment concentration
- Low salinity
- Organic matter not typical for marine environment

## Methods

### Data

Analysis of a long time series Sentinel-2 optical data for the years 2017 – 2018;

### IOPs

Calculation of the Inherent Optical Properties (IOPs) with the Case 2 Regional Coast Colour (C2RCC) processor build in SNAP for complex type 2 waters [1]:

- Output are 5 IOPs – three components for the total absorption – phytoplankton pigment absorption ( $a_{pig}$ ), detritus ( $a_{det}$ ) and gelbstoff / CDOM ( $a_{gelb}$ ) – and two for the scattering – white scatterer ( $b_{wit}$ ), and a typical sediment scatterer ( $b_{part}$ )
- Here is presented the total absorption at 443nm:  $a_{tot} = \text{phytoplankton} + \text{detritus} + \text{CDOM absorption}$  and the percent contribution of each absorber to the total.

### Polygons

IOP data is calculated for each polygon pixel of the study sites, for all acquisition dates available. The values were spatially averaged according to the size of each polygon.

### Meteo data

The IOPs are presented together with meteorological data from ERA5:

- The total precipitation for land sources (riverine and outfall) is cumulative for the last 12 hours before the acquisition time, meridional and zonal mean for the entire area of the Bulgarian coastline. Precipitation data for the study sites in water is hourly value, meridional and zonal mean for the shelf and for the open sea area.
- Wind speed and direction are instantaneous values obtained at acquisition time for the southern and northern land regions, for the shelf area and for open sea.
- Spatial resolution of the ERA5 data is  $0.25^\circ \times 0.25^\circ$ .

## Study area

The study area covers the Bulgarian EEZ of the Black Sea. Altogether 83 positions were pinned, distributed on an even grid on the sea surface. Around each pin a polygon was build, for which surface the IOPs were averaged. The polygons include:

- 12 polygons at river estuaries
- 15 polygons in direct proximity of waste water (WW) treatment plants

There are 56 inwater polygons, positioned at the sea surface with:

- 8 polygons of sea depth below 25m
- 10 polygons of sea depth between 25 and 50m
- 11 polygons of sea depth between 50 and 75m
- 11 polygons of sea depth between 75 and 100m
- 3 polygons of sea depth between 100 and 500m
- 13 polygons of sea depth below 1000m, considered as open sea region

## WW plants

Exact coordinates of the waste water effluents cannot be determined, so the polygons were selected in close proximity to the treatment plant on the sea surface.

## Land sources

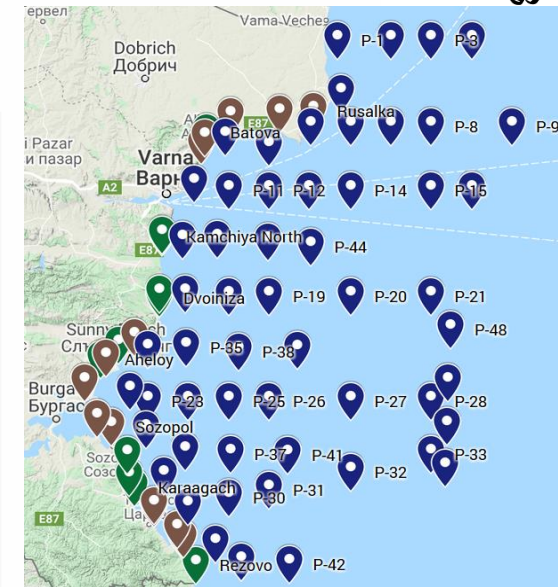
The river estuary and waste water polygons were located ca. 200m from the shoreline so that all polygon pixels are water pixels.

## Polygon surface

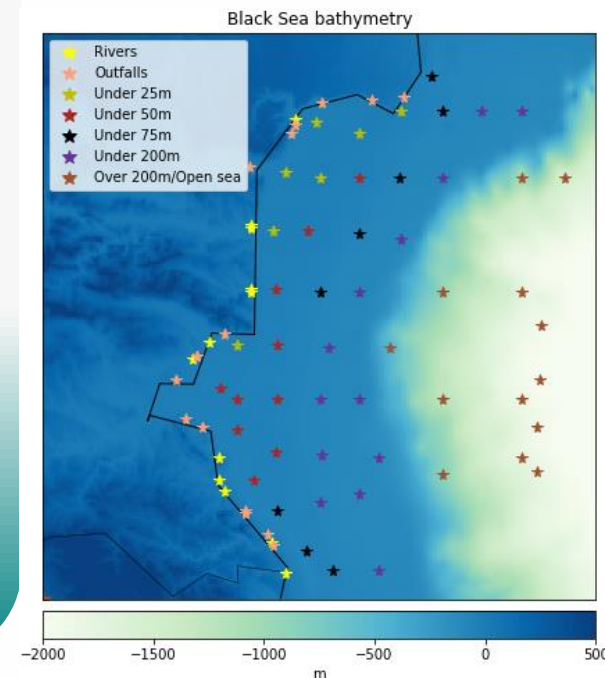
The riverine and outfall polygon size is a circle with radius of  $0.001^\circ$  and that of inwater polygons has a radius of  $0.0025^\circ$ .

## Site map

This is an [interactive map](#) with the exact position of all polygons, their naming and the sea depth for each inwater pin. The bathymetry data is taken from [GEBCO](#) and has a resolution of  $30''$ .



An interactive map of the study area with all coordinates and the depth of each inwater site.



Bathymetry of the study area with grouping of the sites according to their source type and depth.

## Polygons from land sources

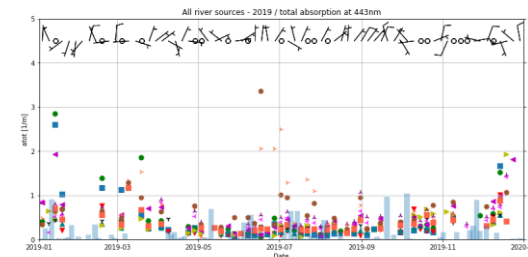
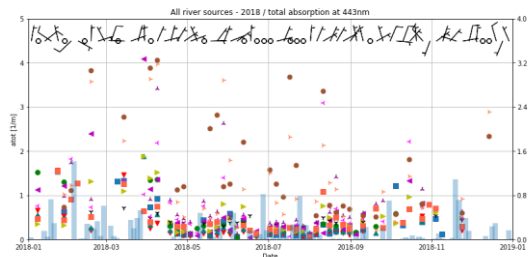
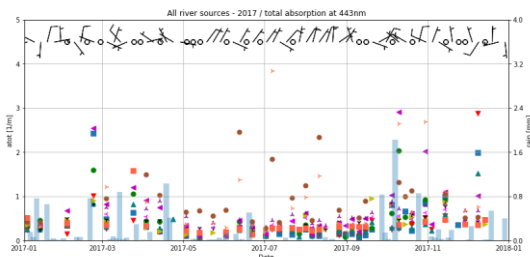
2017

2018

2019

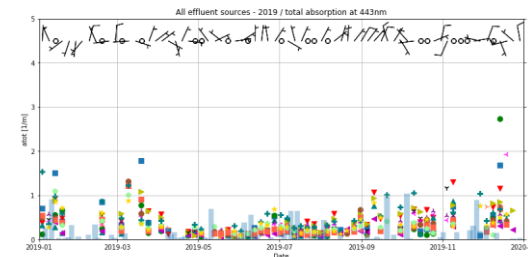
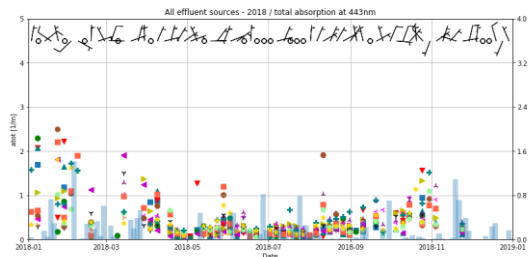
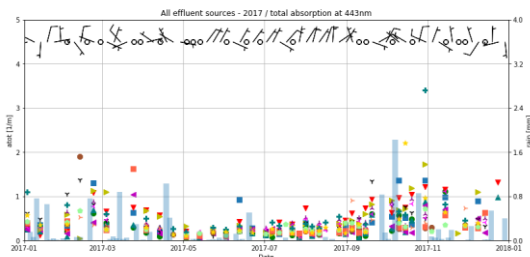
### All river sources

- Rezovo
- Veleka
- ▲ Karaagach
- ▲ Dyavolska
- ▲ Ropotamo
- ▲ Aheloy
- ▲ Hadziska
- ▲ Dvojniza
- ▲ Perperidere
- ▲ Kamchiya North
- ▲ Kamchiya South
- Batova



### All effluent sources

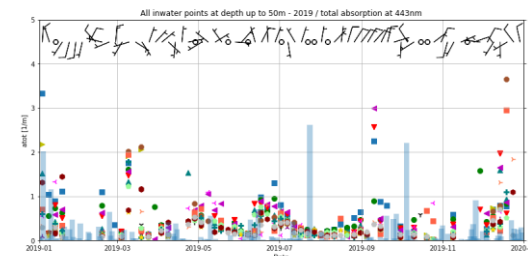
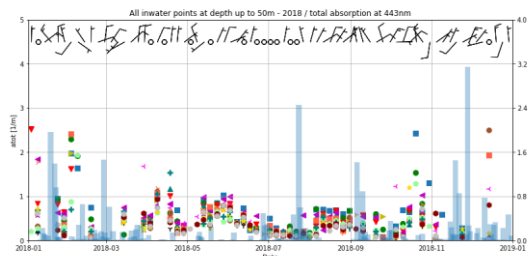
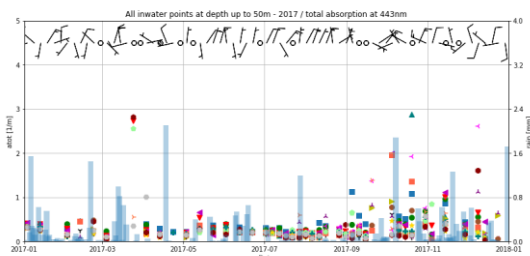
- Sinemorets
- Ahtopol
- Vasiliko
- ▲ Morska Gradina
- ▲ Sozopol
- ▲ Chernomorets
- ▲ Pomorie
- ▲ Aheloy North
- ▲ Aheloy South
- ▲ Elenite
- ▲ ZatiPlyasuci
- ▲ Kranevo
- ▲ Balchik
- ▲ Kavarna
- ▲ Rusalka



## Inwater polygons

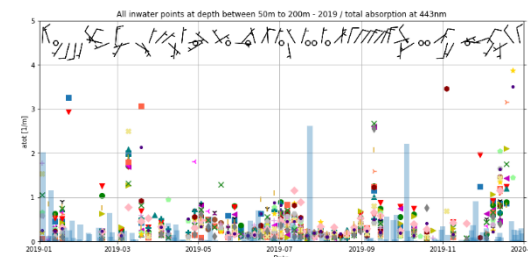
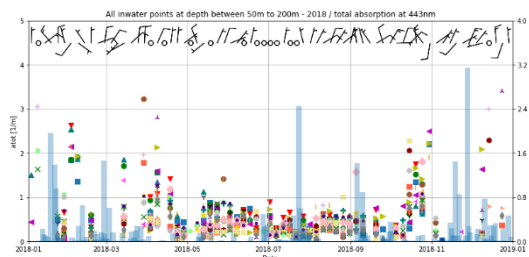
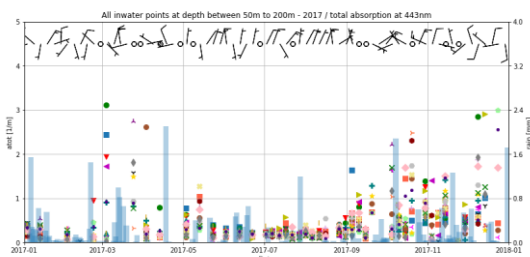
### Inwater points, depth below 50m

- P-1
- P-5
- P-10
- P-11
- P-12
- P-17
- P-22
- P-23
- P-24
- P-34
- P-35
- P-36
- P-50
- P-51
- P-53
- P-54
- P-55



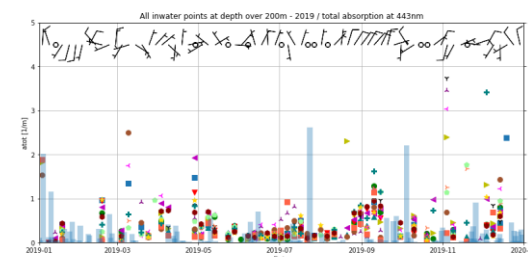
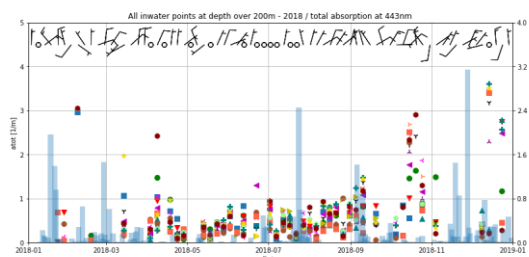
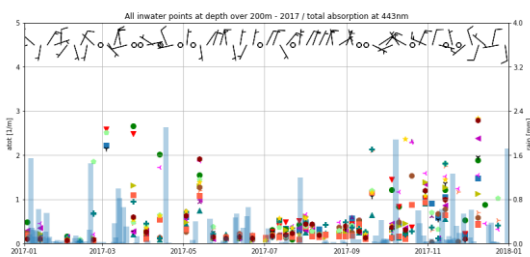
### Inwater points, depth 50m – 100m

- P-2
- P-3
- P-4
- P-6
- P-7
- P-8
- P-13
- P-14
- P-16
- P-19
- P-25
- P-26
- P-29
- P-39
- P-30
- P-31
- P-37
- P-38
- P-40
- P-41
- P-42
- P-44
- P-49
- P-56



### Inwater points, depth 100m – 1500m

- P-9
- P-15
- P-16
- P-20
- P-21
- P-27
- P-28
- P-32
- P-33
- P-43
- P-45
- P-46
- P-47
- P-48





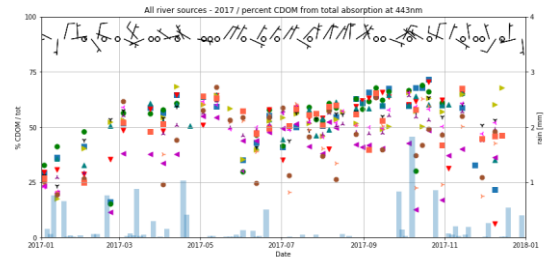
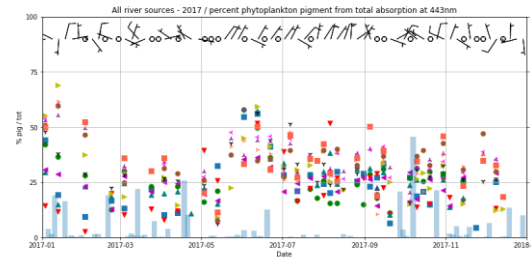
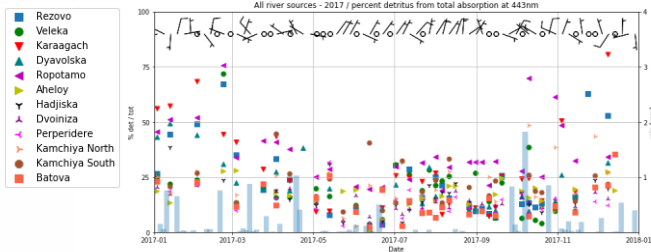
## Polygons from land sources

### Detritus

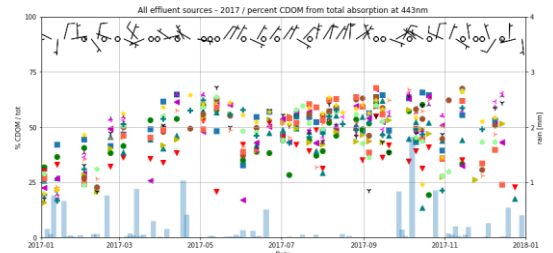
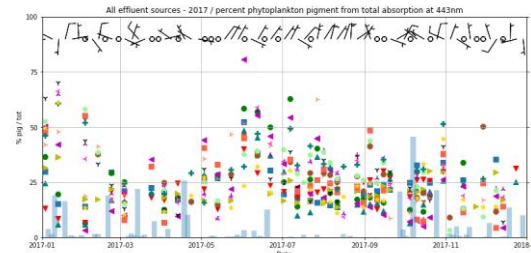
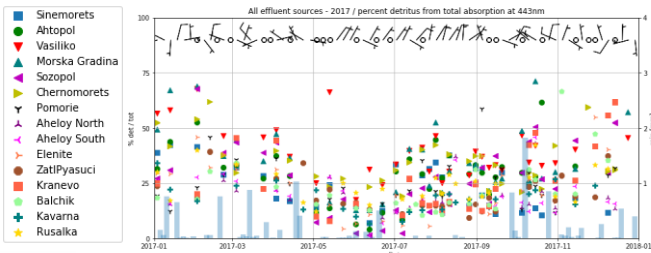
### Phytoplankton pigment

### CDOM

All river sources

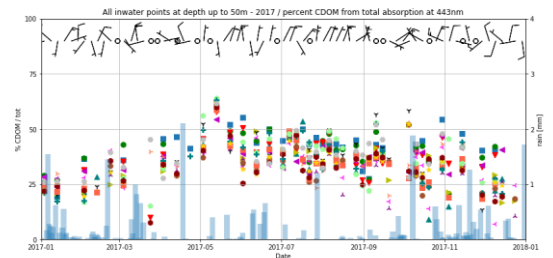
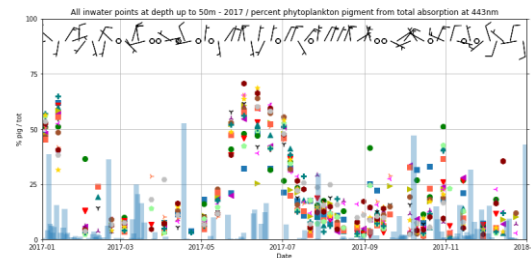
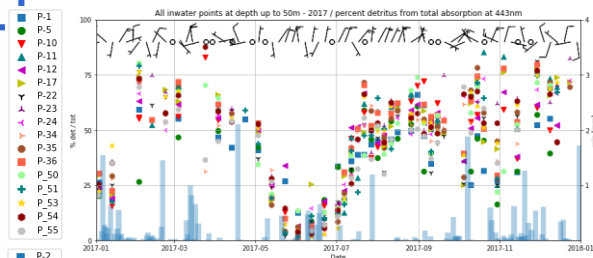


All effluent sources

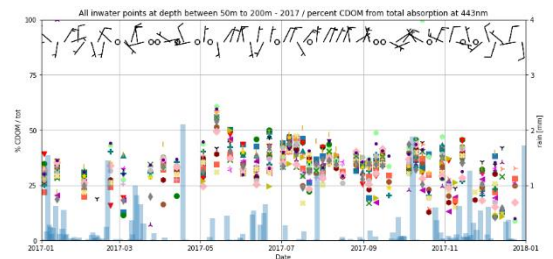
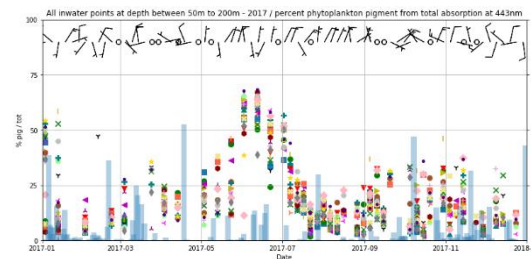
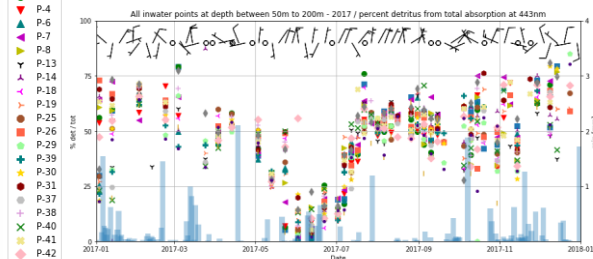


## Inwater polygons

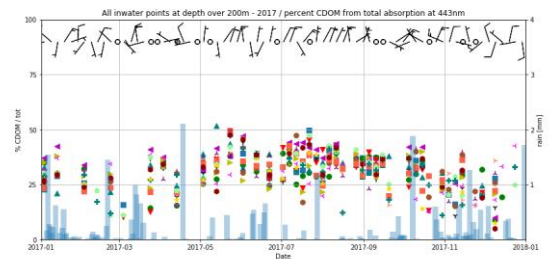
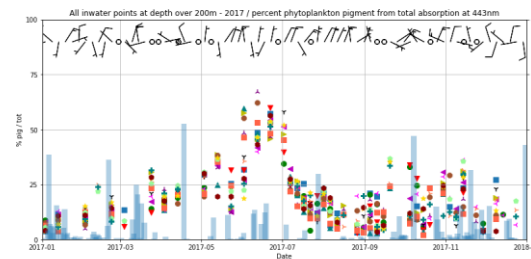
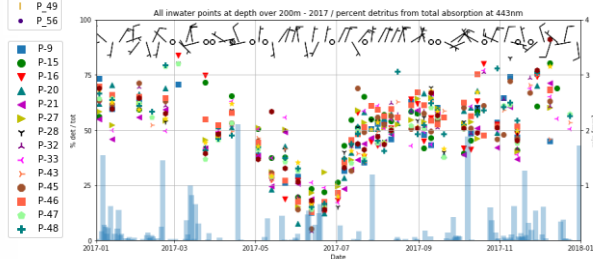
Inwater points, depth below 50m



Inwater points, depth 50m – 100m



Inwater points, depth 100m – 1500m





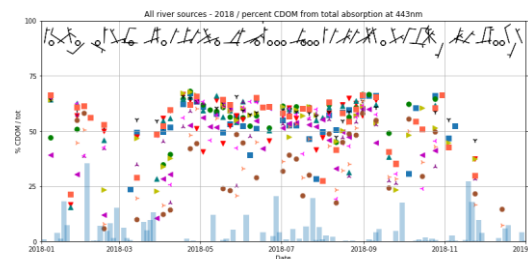
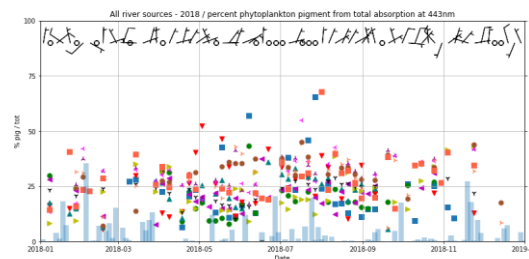
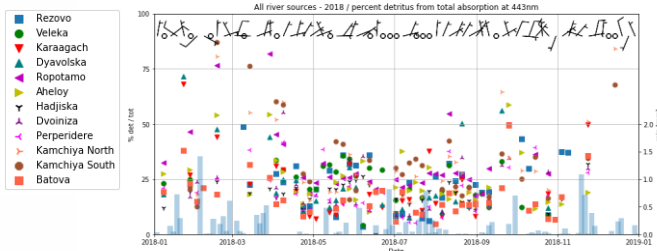
## Polygons from land sources

### Detritus

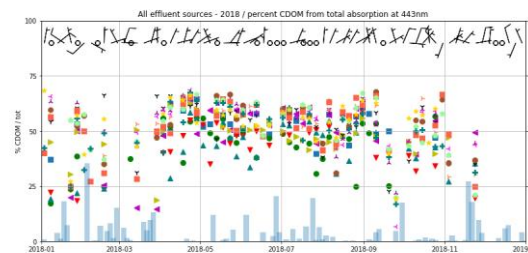
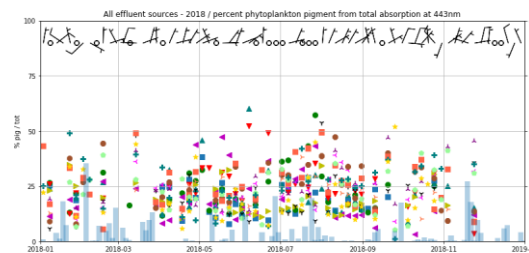
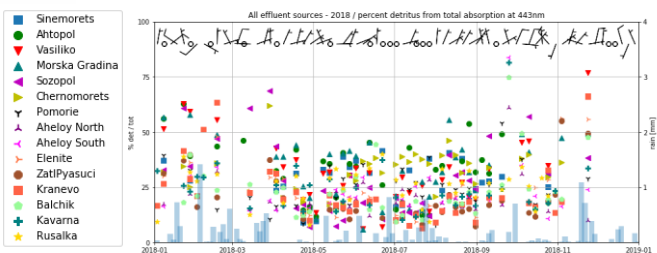
### Phytoplankton pigment

### CDOM

All river sources

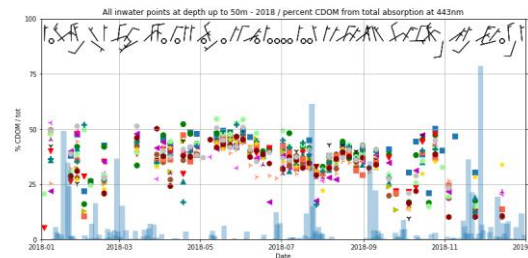
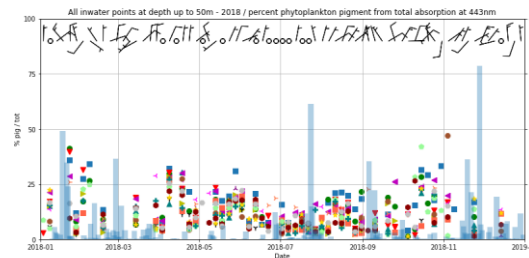
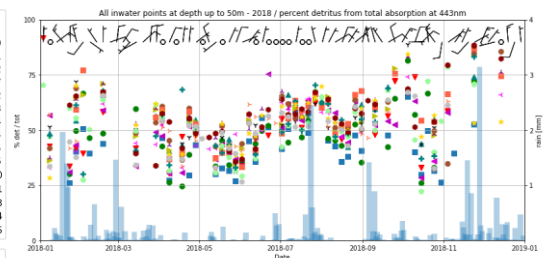


All effluent sources

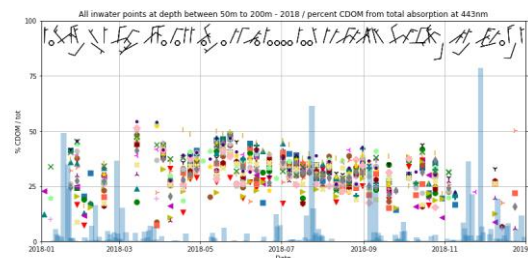
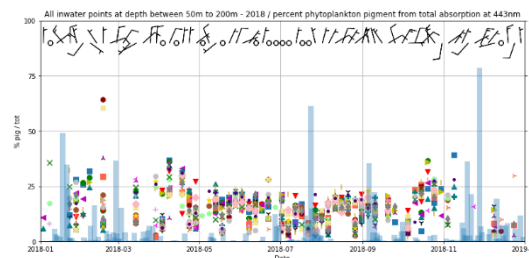
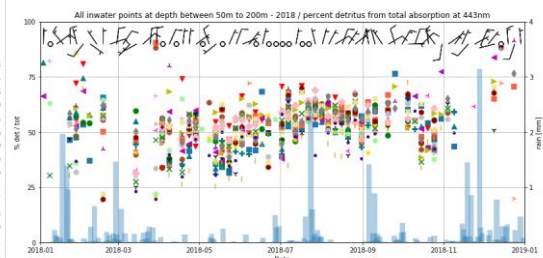


## Inwater polygons

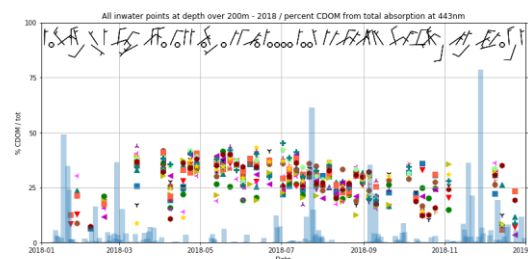
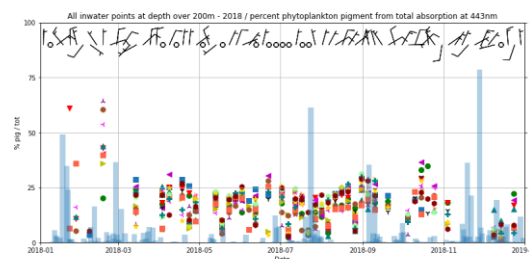
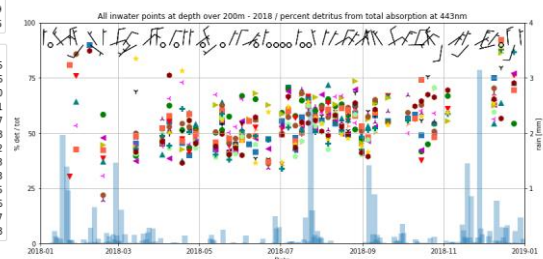
Inwater points, depth below 50m



Inwater points, depth 50m – 100m



Inwater points, depth 100m – 1500m





## Polygons from land sources

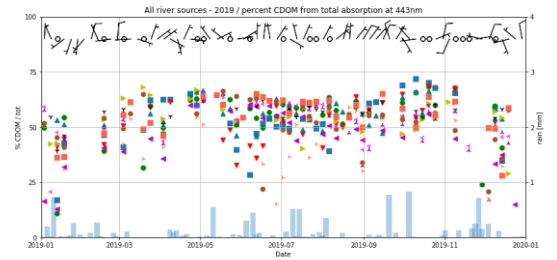
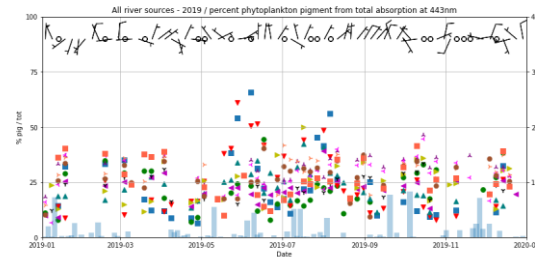
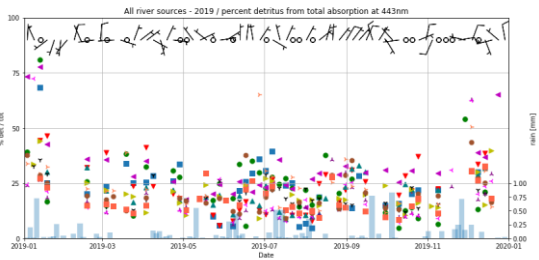
### Detritus

### Phytoplankton pigment

### CDOM

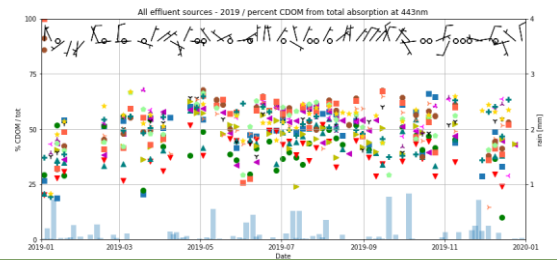
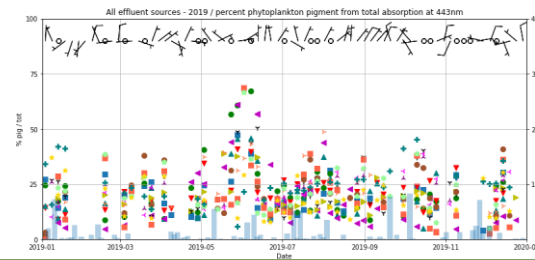
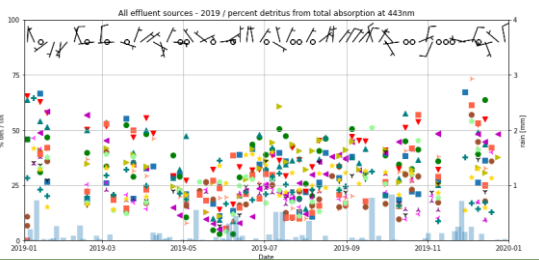
All river sources

- Rezovo
- Veleka
- ▼ Karaagach
- ▲ Dyavolska
- ▼ Ropotamo
- ▲ Aheloy
- ▼ Hadjiska
- ▲ Dvojniza
- ▼ Perperidere
- ▲ Kamchiya North
- ▼ Kamchiya South
- ▲ Batova



All effluent sources

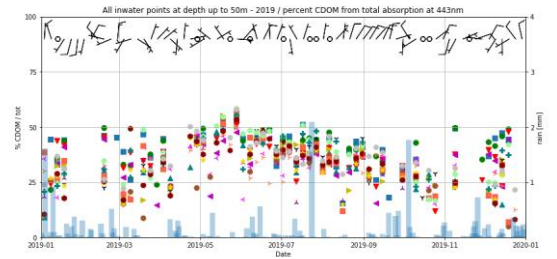
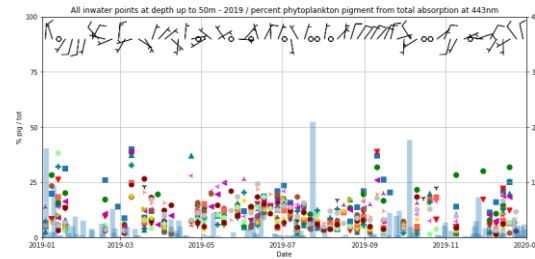
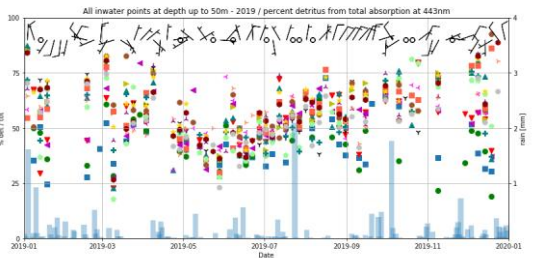
- Sinemorets
- Ahtopol
- ▼ Vasiliko
- ▲ Morska Gradina
- ▼ Sozopol
- ▲ Chernomorets
- ▼ Pomorie
- ▲ Aheloy North
- ▼ Aheloy South
- ▲ Elenite
- ▼ Zlatiplyasuci
- ▲ Kranevo
- ▼ Balchik
- ▲ Kavarna
- ▼ Rusalka



## Inwater polygons

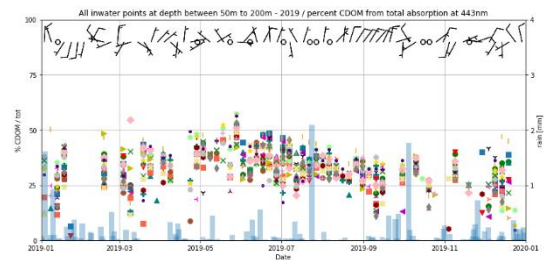
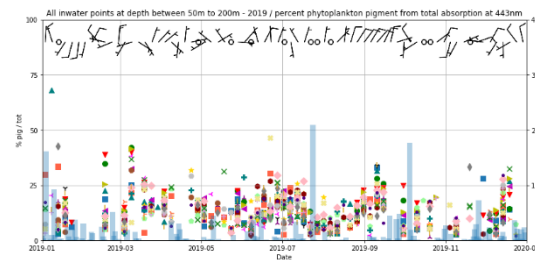
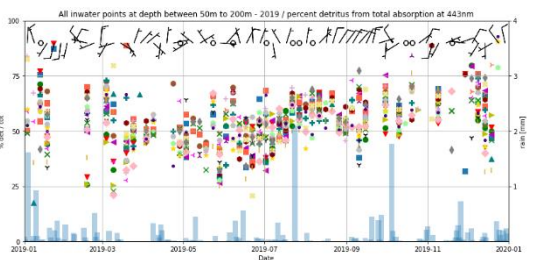
Inwater points, depth below 50m

- P-1
- P-5
- ▼ P-10
- ▲ P-11
- ▼ P-12
- ▲ P-17
- ▼ P-22
- ▲ P-23
- ▼ P-24
- ▲ P-34
- ▼ P-35
- ▲ P-36
- ▼ P-50
- ▲ P-51
- ▼ P-53
- ▲ P-54
- ▼ P-55



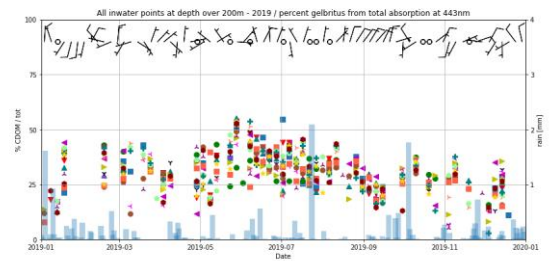
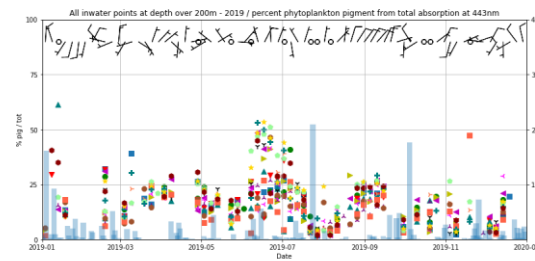
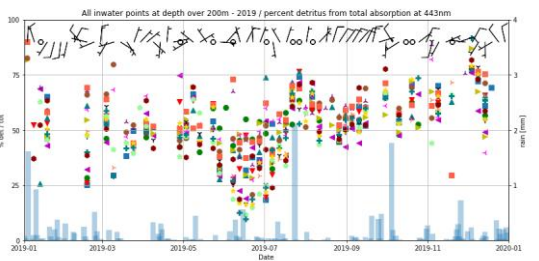
Inwater points, depth 50m – 100m

- P-2
- P-3
- ▼ P-4
- ▲ P-6
- ▼ P-7
- ▲ P-8
- ▼ P-13
- ▲ P-14
- ▼ P-16
- ▲ P-19
- ▼ P-25
- ▲ P-26
- ▼ P-29
- ▲ P-39
- ▼ P-30
- ▲ P-31
- ▼ P-37
- ▲ P-38
- ▼ P-40
- ▲ P-41
- ▼ P-42
- ▲ P-44
- ▼ P-49
- ▲ P-56



Inwater points, depth 100m – 1500m

- P-9
- P-15
- ▼ P-16
- ▲ P-20
- ▼ P-21
- ▲ P-27
- ▼ P-28
- ▲ P-32
- ▼ P-33
- ▲ P-43
- ▼ P-45
- ▲ P-46
- ▼ P-47
- ▲ P-48





## Seasonal trend

- The study sites, chosen close to land sources and those in water areas, regardless the depth of the region they're located, show similar trend in the seasonal fluctuations between each other.
  - There is higher variability between values of the total absorption at 443nm for different sites in the winter/spring and autumn period. These periods correspond to the two phytoplankton blooms, observed with higher intensity in the beginning and lower intensity in the second half of the year, which are typical for the Black Sea region [2].
  - The increase in phytoplankton pigment absorption during the bloom periods is clearly visible on the total value graphs (not shown in this study) and is distinguishable in the graphs showing the percent contribution to total absorption at 443nm.
  - During the summer period the values for all study areas are lower and are in the same range.

## Meteorological conditions

- Prevailing winds for the Bulgarian coastline are North and North-east. A higher variability between the values of the different study sites is connected with change of the wind direction. The highest variability is caused by South winds.
- At very low wind speed or windless conditions the IOPs for all study sites show similar values.
- Overall after prolonged precipitation there is an increase in the range between the values of all observed sites.

## References

- [1] Brockmann, C., Doerffer, R., Peters, M., Kerstin, S., Embacher, S., & Ruescas, A. (2016). Evolution of the C2RCC neural network for Sentinel 2 and 3 for the retrieval of ocean colour products in normal and extreme optically complex waters. In *Living Planet Symposium* (Vol. 740, p. 54).
- [2] Chu, P. C., Ivanov, L. M., & Margolina, T. M. (2005). Seasonal variability of the Black Sea chlorophyll-a concentration. *Journal of Marine Systems*, 56(3-4), 243-261.

## Percent contribution of each absorber to the total

- CDOM is the main absorber for the study sites connected with land sources. For those regions it counts for over 50% of the total absorption at 443nm. CDOM absorption at inwater sites has a comparatively lower impact. Its ratio is less than 50% of the total.
- The phytoplankton pigment absorption has the smallest percent contribution to the total absorption at 443nm, except for the period late May, beginning of July, when the ratio  $a_{pig}/a_{tot}$  has a peak. A noticeable increase of this ratio is also observed during the bloom period in winter/spring and autumn.
- Detritus absorption for land sources counts for less than 50% of the total absorption. For inwater areas this ratio increases, making up to over 55-60% of the total. A minimum in the ratio  $a_{det}/a_{tot}$  is observed for the late May, beginning of June, connected with the phytoplankton pigment peak.
- The phytoplankton absorption peak of  $a_{pig}/a_{tot}$  is compensated by a low in the detritus absorption. The peak is present for all sources, however it's more prominent for inwater sites. It's visible for all years, showing lowest amplitude in 2018. The CDOM absorption ratio shows little variation throughout the year, compared to the other two variables.

## Conclusions

- The trends observed in this study confirm that the predominant absorber for the Black Sea region is CDOM. The peak in phytoplankton pigment absorption during the spring is compensated mainly by detritus. The main source of nutrients, necessary for the phytoplankton growth is the river inflow, which intensifies during the spring period. The phytoplankton absorption peak has lower amplitude at study sites in river and effluent areas compared to the inwater regions, as river plumes and effluent discharges are sources of optically active absorbers, which increase the CDOM and detritus contribution in those regions.
- The IOPs for sites connected with land sources and inwater sites show similar behaviour, however they are distinguishable according to the impact of each absorber to the total absorption. Monitoring this change can serve as an indicator of the impact of the fluvial plume away from the shoreline. According to our observations effluent plumes demonstrate similar behaviour as fluvial sources.
- The most prominent technique for detection of riverine outflow in the sea seems to be the increased fraction of CDOM contribution to the total absorption at 443 nm and the lower phytoplankton contribution.
- The high variability between the values for the various study sites during the bloom period indicates the strong influence of the local circulation.

## Acknowledgments

We would like to acknowledge ESA-RSS (Research and Service Support), and in particular G. Sabatino and R. Cuccu for their assistance in processing the data with [G-POD](#).